PROCEEDINGS OF SPIE

SPIEDigitalLibrary.org/conference-proceedings-of-spie

# Spatio-temporal activity in cortical network during cognitive activity

Kuc, Alexander, Malova, Natalija, Maksimenko, Vladimir

Alexander Kuc, Natalija Malova, Vladimir Maksimenko, "Spatio-temporal activity in cortical network during cognitive activity," Proc. SPIE 11459, Saratov Fall Meeting 2019: Computations and Data Analysis: from Nanoscale Tools to Brain Functions, 1145907 (9 April 2020); doi: 10.1117/12.2563871

Event: Saratov Fall Meeting 2019: VII International Symposium on Optics and Biophotonics, 2019, Saratov, Russian Federation

# Spatio-temporal activity in cortical network during cognitive activity

Alexander Kuc, Natalija Malova, Vladimir Maksimenko

Neuroscience and Cognitive Technology Laboratory, Center for Technologies in Robotics and Mechatronics Components, Innopolis University, Universitetskaya St, 1, Innopolis, Tatarstan 420500, Russia

## ABSTRACT

It is known that brain performs cognitive functions through the activation of a distributed cortical network, which includes remote cortical regions. With this in mind we have analyzed the spatio-temporal cortical activity based on multichannel EEG recordings during accomplishing cognitive task. As the result, we have revealed typical spatio-temporal structures related to the different levels of cognitive task complexity.

**Keywords:** signal analysis, visual stimuli, cognitive load

## 1. INTRODUCTION

The study of brain activity during the accomplishing of cognitive tasks is one of the most interesting and challenging topics in neuroscience. Different features of the neuronal activity are known to be associated with the complex psychophysiological processes and cognitive functions, such as attention,[1] memory,[2] intelligence,[3] decision-making.[4] The neuronal activity features can be studied with the help of noninvasive techniques, e.g. electroencephalography (EEG) and magnetoencephalography (MEG). For instance, the recent works reported the classification of brain states associated with the state of uncertainty and decision-making by using MEG.[5] Also, recent work described the analysis of human motivation based on the consideration of EEG trials.[6] The reported possibility to use noninvasive EEG recordings for the human condition evaluation is important for the development of the brain-computer interfaces (BCI) enabling the monitoring and control of the brain states.[7,8] The recorded EEG signals consist of the different rhythms and the brain noise[9] that take part in the formation of certain cognitive functions. During the accomplishing of the complex cognitive tasks, a distributed functional cortical network is activated, involving the neurons from various remote areas of the brain and synchronize their activity in the different frequency bands.[10,11]

In this work we performed a spatio-temporal analysis of the cortical activity in the $\alpha$- and $\beta$-frequency bands during the cognitive task accomplishing. The cognitive task implied a classification of the ambiguous visual stimuli (Necker cubes) according to their interpretations. This task is the example of a decision-making task which requires the subject to make a decision based on the available sensory information. Usually, the perceptual decision-making task is not viewed as a classical cognitive domain like attention or memory. At the same time, this is mostly true for near-threshold stimuli[12] or unambiguous stimuli. In our experiments, we used ambiguous visual stimuli,whose classification caused uncertainty in decision-making when ambiguity is high.[5] Finally, in agreement with the recent work,[4] the Necker cube interpretation was considered as a cognitive decision process. The choice of the $\alpha$- and $\beta$-frequency bands was attributable to their established role in the sensory information processing[13] and decision-making.[14]

Further author information: (Send correspondence to V. Maksimenko)
V. Maksimenko: E-mail: maximenkovl@gmail.com, Telephone: +7 905 324 8118

Saratov Fall Meeting 2019: Computations and Data Analysis: from Nanoscale Tools to Brain Functions, edited by Dmitry E. Postnov, Proc. of SPIE Vol. 11459, 1145907 · © 2020 SPIE
CCC code: 1605-7422/20/$21 · doi: 10.1117/12.2563871

## 2. METHODS

### 2.1 Experimental procedure

Ten healthy subjects (5 males and 5 females), between the ages of 26 and 35 with normal or corrected-to-normal visual acuity participated in the experiments. All of them provided informed written consent before participating in the experiment. The experimental studies were performed in accordance with the Declaration of Helsinki and approved by the local research ethics committee of the Innopolis University.

The Necker cube was used as the visual stimuli.[15] It represents itself a cube with transparent faces and visible edges; an observer without any perception abnormalities sees the Necker cube as a 3D-object due to the specific position of the cube's edges. Bistability in perception consists in the interpretation of this 3D-object as to be either left- or right-oriented depending on the constrast of different inner edges of the cube. The contrast $a \in [0, 1]$ of the three middle lines centered in the left middle corner was used as a control parameter. The values $a = 1$ and $a = 0$ correspond, respectively, to 0 (black) and 255 (white) pixels' luminance of the middle lines. If $a$ is close to 0 or 1, such a Necker cube is easily interpreted as either right-oriented or left-oriented. For $a \sim 0.5$, identifying the orientation of the Necker cube becomes difficult, since such an image has a high level of ambiguity. During the experiment, the subject was randomly shown 400 cubes of Necker with different values of the parameter $a$.

Participants of the experiment were instructed to press either the left or right key depending on the first impression of the orientation of the Necker cube. Since the perception of the current cube can be influenced by previously demonstrated Necker cubes, the length of the visual stimulus representation varied in the range of $1 - 1.5$ s. Also, a random change in the control parameter $a$ also prevented the stabilization of perception. In addition, abstract images were exhibited for about $\gamma = 3.0 - 5.0$ between demonstrations of the Necker cube image to eliminate the "memory effect".

The EEG signals were recorded using the monopolar registration method and the classical extended ten–ten electrode system. We recorded 31 signals with two reference electrodes A1 and A2 on the earlobes and a ground electrode N just above the forehead. The signals were acquired via the cup adhesive Ag/AgCl electrodes placed on the "Tien–20" paste (Weaver and Company, Colorado, USA). Immediately before the experiments started, we performed all necessary procedures to increase skin conductivity and reduce its resistance using the abrasive "NuPrep" gel (Weaver and Company, Colorado, USA). The impedance was monitored after the electrodes were installed and measured throughout the experiments. Usually, the impedance values varied within a 2–5 kΩ interval. The electroencephalograph "Encephalan-EEG-19/26" (Medicom MTD company, Taganrog, Russian Federation) with multiple EEG channels and a two-button input device (keypad) was used for amplification and analog-to-digital conversion of the EEG signals. The raw EEG signals were filtered by a band-pass filter with cut-off points at 1 Hz (HP) and 100 Hz (LP) and by a 50-Hz notch filter by embedded a hardware-software data acquisition complex.

### 2.2 Signal analysis

We analyzed the EEG signals power in $\alpha$- and $\beta$-frequency bands, using the continuous wavelet transformation. The wavelet power spectrum $E^n(f, t) = (W^n(f, t))^2$ was calculated for each EEG channel $X_n(t)$ in the frequency range $1 - 30$ Hz including both $\alpha$ and $\beta$ ranges. Here, $W^n(f, t)$ is the complex-valued wavelet coefficients calculated as

$$W^n(f,t) = \sqrt{f} \int_{t-4/f}^{t+4/f} X_n(t)\psi^*(f,t)dt, \tag{1}$$

where $n = 1, ..., N$ is the EEG chanel number ($N = 31$ is the total number of chanels used for the analysis) and "*" defines the complex conjugation. The mother wavelet function $\psi(f, t)$ is the Morlet wavelet[16] which is defined as

$$\psi(f,t) = \sqrt{f}\pi^{1/4}\mathrm{e}^{j\omega_0 f(t-t_0)}\mathrm{e}^{f(t-t_0)^2/2}, \tag{2}$$

where $\omega_0 = 2\pi$ is the wavelet parameter.[17]

For $\alpha$- and $\beta$-frequency bands the wavelet amplitudes $E^n_\alpha(t)$ and $E^n_\beta(t)$ were calculated as

$$E^n_{\alpha,\beta}(t) = \frac{1}{\Delta f_{\alpha,\beta}} \int\limits_{\Delta f_{\alpha,\beta}} E^n(f', t)df', \tag{3}$$

where $\Delta f_\alpha = 8 - 12$ Hz, $\Delta f_\beta = 15 - 30$ Hz. The time-series of the wavelet power (3) was calculated for the whole time of the experimental session and then was split into the time segments $\tau^i_{\text{pre}} = 0.5$ s and $\tau^i_{\text{post}} = 0.5$ s, before and after the $i$-th visual stimulus presentation.

$$\langle E^n_{\alpha,\beta} \rangle_{\tau^i_{\text{pre}},\tau^i_{\text{post}}} = \int\limits_{\tau^i_{\text{pre}},\tau^i_{\text{post}}} E^n_{\alpha,\beta}(t')dt'. \tag{4}$$

For each stimulus ambiguity the difference between $\langle E^n_{\alpha,\beta} \rangle_{\tau^i_{\text{pre}}}$ and $\langle E^n_{\alpha,\beta} \rangle_{\tau^i_{\text{post}}}$ for the $n$-th EEG sensor was analyzed statistically via the paired samples t-test based on 20 trials.

## 3. RESULTS

In the framework of this study, the complexity of the considered task was associated with the ambiguity of the visual stimulus. To investigate the effect of visual stimulus complexity, all Necker cubes were divided into two groups (each group included 80 stimuli - 20 for each value of parameter $a$):

- Low ambiguity (LA) stimuli, including the Necker cube images with $a \in \{0.15, 0.25, 0.75, 0.85\}$
- High ambiguity (HA) stimuli, including the Necker cube images with $a \in \{0.40, 0.45, 0.55, 0.60\}$

Changes in electrical activity of the brain induced by the visual sensory information processing were analyzed (see methods) and the EEG channels showing significant changes (increase or decrease) in spectral energy in the alpha and beta frequency ranges were identified. Figure 1 shows the difference $D$ between the number of EEG channels where $E_\alpha$ increases and those where $E_\alpha$ decreases for LA and HA stimuli after the presentation of the visual stimulus.

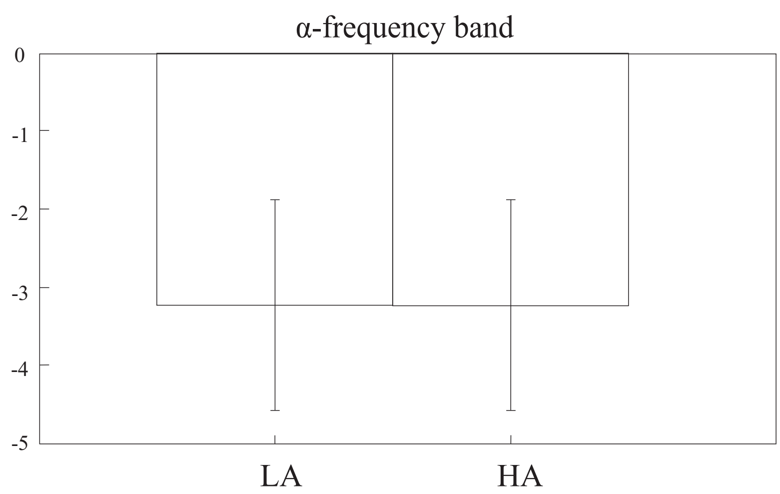


Figure 1. Difference $D$ (group mean±SE) between the number of EEG channels, where $\alpha$-band energy ($E_\alpha$) increases and those where $E_\alpha$ decreases versus stimuli ambiguity (LA, HA)

The median values of $D = -1.75$ for LA stimuli and $D = -2.5$ for HA stimuli, indicating a predominance of EEG channels in which energy of the $\alpha$-band decreases after presentation of the visual stimulus.

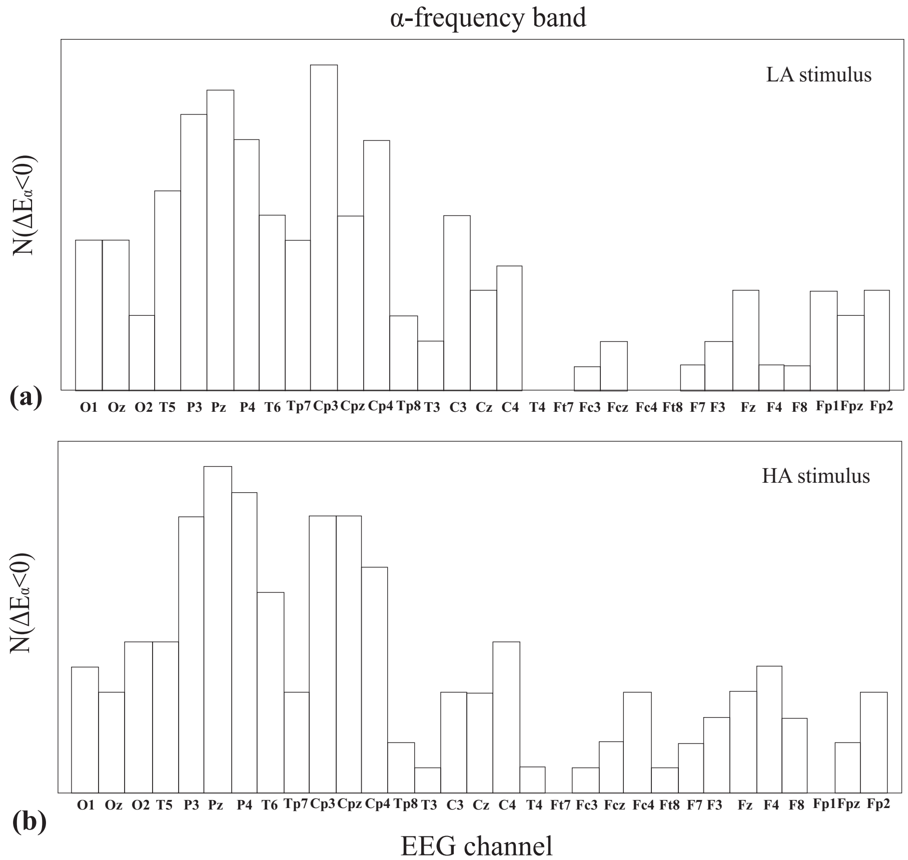


Figure 2. Plot of EEG channels (group mean) reflecting $E_\alpha$ decrease for all subjects for LA (a) and HA (b) stimuli

A repeated measures ANOVA is used to compare the differences of $D$ between time points (before and after the presentation of the visual stimulus), as well as for the level of ambiguity of the images presented (LA and HA). ANOVA with Greenhouse-Geissser correction shows a significant difference in the value of $D$ after the stimulus is demonstrated relative to the value of $D$ before the image is presented ($F_{1,9} = 8.28, p = 0.018$) however the difference between LA and HA stimuli is negligible ($F_{1,9} = 0.25, p = 0.877$). Wilcoxon signed rank test for the related samples did not revealed significant change between LA and RA groups.

Therefore, after the presentation of the visual stimulus, the number of channels showing a decrease of energy in the $\alpha$ range increases regardless of the level of ambiguity of the stimulus, which indicates a decrease of the activity in the $\alpha$ range during the processing of visual information.

Figure 2 shows EEG channels exhibiting the effect of decreasing alpha-band activity for LA (a) and HA (b) stimuli after presentation of the visual stimulus. The higher value of $N$ means that more subjects show a decrease in the energy of the $\alpha$-range in this particular area. It can be seen that the distribution reaches the highest values for the parietal region (P3, Pz, P4).

Then we have considered the energy changes in the $\beta$-range. Figure 3 shows the difference $D$ between the number of EEG channels where $E_\beta$ increases and those where $E_\beta$ decreases for LA and HA stimuli after presentation of the visual stimulus.

Wilcoxon signed rank test for related samples shown significantly changes for LA and HA after visual stimulus demonstration ($p = 0.032$). Thus, according to our results, unlike $\alpha$-band energy, the energy in $\beta$-band changes in different way for different stimuli ambiguity. For HA stimuli, the number of channels demonstrating increase of $\beta$-band energy exceeds one corresponding to LA stimuli.

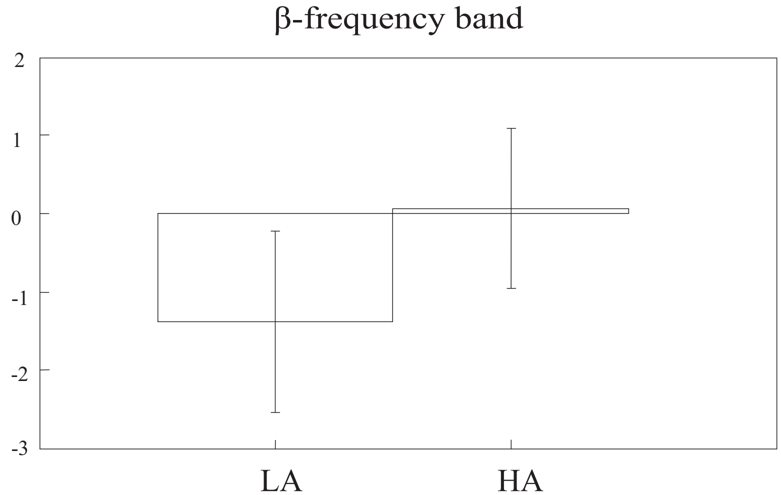


Figure 3. Difference $D$ (group mean±SE) between the number of EEG channels, where $\beta$-band energy ($E_\beta$) increases and those where $E_\beta$ decreases versus stimuli ambiguity (LA, HA)

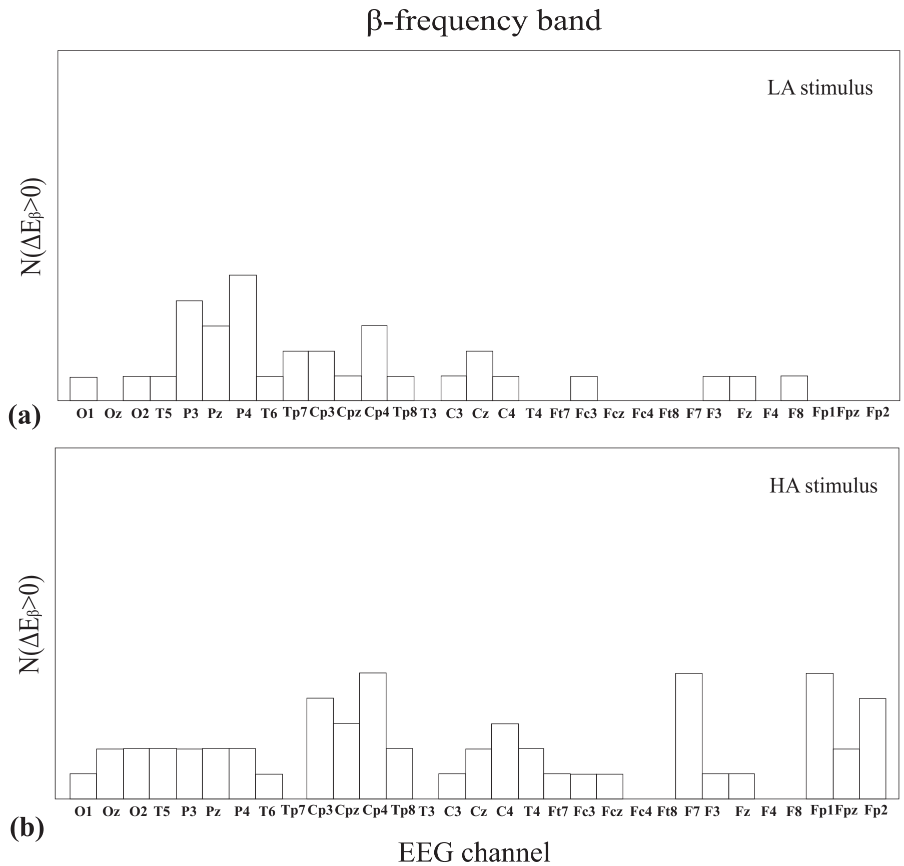


Figure 4. Plot of EEG channels (group mean) reflecting $E_\beta$ increase for all subjects for LA (a) and HA (b) stimuli

In addition, for the ambiguity of the visual stimulus, the localization of EEG channels demonstrating an increase in energy in the beta range is different (Figure 4). For LA stimuli (b) $\beta$-band energy increases in the parietal area (P3, Pz, P4 EEG channels). For HA stimuli (c) the $\beta$-band energy increases mostly in frontal area (Fp1, Fpz, Fp2 EEG channels), as well as in parietal area (Cp3, Cpz, Cp4 EEG channels).

## 4. CONCLUSION

The features of neural activity of the brain in the $\alpha$- and $\beta$-frequency band during the processing of visual information of varying complexity were analyzed. During the analysis, it was found that the behavior of the $\alpha$-rhythm remains unchanged for both simple visual stimuli and complex ones and consists in the destruction of the $\alpha$-rhythm energy in the parietal region of the brain. Unlike the dynamics of the $\alpha$-rhythm, the behavior of the $\beta$-rhythm differs when processing visual information of varying complexity. When processing visual information with a low level of ambiguity, there is an increase of $\beta$-rhythm energy in the parietal area. When processing visual information with a high level of ambiguity, $\beta$-rhythm energy increased in the frontal and parietal areas of the brain.

## 5. ACKNOWLEDGMENTS

This work has been supported by the Russian Science Foundation (project No 19-12-00050)

## REFERENCES


[1] Maksimenko, V. A., Runnova, A. E., Frolov, N. S., Makarov, V. V., Nedaivozov, V., Koronovskii, A. A., Pisarchik, A., and Hramov, A. E., "Multiscale neural connectivity during human sensory processing in the brain," *Physical Review E* **97**(5), 052405 (2018).

[2] Onton, J., Delorme, A., and Makeig, S., "Frontal midline eeg dynamics during working memory," *Neuroimage* **27**(2), 341–356 (2005).

[3] Maksimenko, V. A., Runnova, A. E., Zhuravlev, M. O., Protasov, P., Kulanin, R., Khramova, M. V., Pisarchik, A. N., and Hramov, A. E., "Human personality reflects spatio-temporal and time-frequency eeg structure," *PloS one* **13**(9), e0197642 (2018).

[4] Maksimenko, V. A., Frolov, N. S., Hramov, A. E., RUNNOVA, A. E., Grubov, V. V., Kurths, J., and Pisarchik, A. N., "Neural interactions in a spatially-distributed cortical network during perceptual decision-making," *Frontiers in behavioral neuroscience* **13**, 220 (2019).

[5] Hramov, A. E., Frolov, N. S., Maksimenko, V. A., Makarov, V. V., Koronovskii, A. A., Garcia-Prieto, J., Antón-Toro, L. F., Maestú, F., and Pisarchik, A. N., "Artificial neural network detects human uncertainty," *Chaos: An Interdisciplinary Journal of Nonlinear Science* **28**(3), 033607 (2018).

[6] Maksimenko, V. A., Runnova, A. E., Zhuravlev, M. O., Makarov, V. V., Nedayvozov, V., Grubov, V. V., Pchelintceva, S. V., Hramov, A. E., and Pisarchik, A. N., "Visual perception affected by motivation and alertness controlled by a noninvasive brain-computer interface," *PloS one* **12**(12), e0188700 (2017).

[7] Maksimenko, V. A., Hramov, A. E., Grubov, V. V., Nedaivozov, V. O., Makarov, V. V., and Pisarchik, A. N., "Nonlinear effect of biological feedback on brain attentional state," *Nonlinear Dynamics* **95**(3), 1923–1939 (2019).

[8] Maksimenko, V. A., Hramov, A. E., Frolov, N. S., Lüttjohann, A., Nedaivozov, V. O., Grubov, V. V., Runnova, A. E., Makarov, V. V., Kurths, J., and Pisarchik, A. N., "Increasing human performance by sharing cognitive load using brain-to-brain interface," *Frontiers in neuroscience* **12** (2018).

[9] Pisarchik, A. N., Chholak, P., and Hramov, A. E., "Brain noise estimation from meg response to flickering visual stimulation," *Chaos, Solitons & Fractals: X* **1**, 100005 (2019).

[10] Makarov, V. V., Zhuravlev, M. O., Runnova, A. E., Protasov, P., Maksimenko, V. A., Frolov, N. S., Pisarchik, A. N., and Hramov, A. E., "Betweenness centrality in multiplex brain network during mental task evaluation," *Physical Review E* **98**(6), 062413 (2018).

[11] Frolov, N. S., Maksimenko, V. A., Khramova, M. V., Pisarchik, A. N., and Hramov, A. E., "Dynamics of functional connectivity in multilayer cortical brain network during sensory information processing," *The European Physical Journal Special Topics* **228**(11), 2381–2389 (2019).

[12] Weisz, N., Wühle, A., Monittola, G., Demarchi, G., Frey, J., Popov, T., and Braun, C., "Prestimulus oscillatory power and connectivity patterns predispose conscious somatosensory perception," *Proceedings of the National Academy of Sciences* **111**(4), E417–E425 (2014).

[13] Michalareas, G., Vezoli, J., Van Pelt, S., Schoffelen, J.-M., Kennedy, H., and Fries, P., "Alpha-beta and gamma rhythms subserve feedback and feedforward influences among human visual cortical areas," *Neuron* **89**(2), 384–397 (2016).

[14] Chand, G. B. and Dhamala, M., "Interactions between the anterior cingulate-insula network and the fronto-parietal network during perceptual decision-making," *Neuroimage* **152**, 381–389 (2017).

[15] Kornmeier, J., Friedel, E., Wittmann, M., and Atmanspacher, H., "Eeg correlates of cognitive time scales in the necker-zeno model for bistable perception," *Consciousness and cognition* **53**, 136–150 (2017).

[16] Pavlov, A. N., Hramov, A. E., Koronovskii, A. A., Sitnikova, E. Y., Makarov, V. A., and Ovchinnikov, A. A., "Wavelet analysis in neurodynamics," *Physics-Uspekhi* **55**(9), 845 (2012).

[17] Sitnikova, E., Hramov, A. E., Grubov, V., and Koronovsky, A. A., "Time-frequency characteristics and dynamics of sleep spindles in wag/rij rats with absence epilepsy," *Brain Research* **1543**, 290–299 (2014).